Journal of Macromolecular Science, Part A
Publication details, including instructions for authors and subscription information:
http://www.informaworld.com/smpp/title~content=t713597274

Synthesis and Characterization of PS-PIB-PS Triblock Copolymers

Robson F. Storey[a]; Bret J. Chisholm[b]; Kim R. Choate[a]
[a] Department of Polymer Science, The University of Southern Mississippi, Hattiesburg, Mississippi [b] The General Electric Company, Mount Vernon, Indiana

To cite this Article Storey, Robson F. , Chisholm, Bret J. and Choate, Kim R.(1994) 'Synthesis and Characterization of PS-PIB-PS Triblock Copolymers', Journal of Macromolecular Science, Part A, 31: 8, 969 — 987
To link to this Article: DOI: 10.1080/10601329409349773
URL: http://dx.doi.org/10.1080/10601329409349773

J.M.S.—PURE APPL. CHEM., A31(8), pp. 969–987 (1994)

SYNTHESIS AND CHARACTERIZATION OF PS-PIB-PS TRIBLOCK COPOLYMERS

ROBSON F. STOREY,* BRET J. CHISHOLM,† and KIM R. CHOATE

Department of Polymer Science
The University of Southern Mississippi
Hattiesburg, Mississippi 39406-0076

ABSTRACT

Poly(styrene–isobutylene–styrene) (PS–PIB–PS) block copolymers synthesized via living carbocationic polymerization using a di- or tricumyl chloride/$TiCl_4$/pyridine initiating system in 60/40 (v/v) hexane/methyl chloride cosolvents. The kinetics of formation of the PIB block at −80°C were found to be first order in isobutylene (IB) concentration, first order in the concentration of initiating sites, second order in $TiCl_4$ concentration, and a negative fractional order with respect to the pyridine concentration. The rate of polymerization was found to decrease with increasing temperature, indicating an equilibrium between dormant, covalent and active, ionized chain ends, and chain-end concentration studies suggested that there was no contribution by free ions to the rate of propagation. Diagnosis of the livingness of the IB polymerization indicated that at high (≥90%) monomer conversion, β-proton elimination becomes important, causing the timing of addition of styrene to be critical. Addition of styrene at an IB reaction time significantly exceeding the time necessary for complete IB consumption resulted in contamination of the product with a substantial amount of homo-PS; conversely, addition at intermediate IB conversion resulted in slow copolymerization between IB and styrene and the formation of a tapered block copolymer. Addition of styrene at an IB conversion of about 90% resulted in well-defined block copolymers which displayed ordered, phase-separated

†Present address: The General Electric Company, Mount Vernon, Indiana 47620-9364.

morphologies consisting of cylinders of PS in a continuous phase of PIB. The block copolymers possessed properties consistent with those of physically crosslinked rubbers. Dynamic mechanical spectroscopy revealed two glass transitions with a broad rubbery plateau extending from about 0 to 100°C, and tensile strengths of up to 25 MPa and elongations to 1000% were observed for some samples.

INTRODUCTION

Thermoplastic elastomers (TPEs) consist of flexible polymer chains that are physically rather than covalently chemically crosslinked, and thus possess many of the properties of vulcanized rubbers, but may be melt processed at elevated temperatures using conventional polymer processing equipment. Examples of TPEs are elastomeric ionomers [1, 2] and A–B–A block copolymers [3]. The latter TPEs are produced commercially via living anionic polymerization using a sequential monomer addition technique, and are typically based on polydiene center blocks and polystyrene (PS) outer blocks. A disadvantage of the diene-based inner block is its inherent tendency toward oxidation and ozonation; hydrogenated versions are available commercially, for example Kraton G [4], but this modification is relatively costly. In comparison, a TPE based on a polyisobutylene (PIB) soft segment would be inherently fully saturated, and would be expected to provide superior oxidative, chemical, and thermal stability. In addition, for certain applications, PIB-based triblocks would yield barrier and damping properties that cannot be obtained with diene-based materials.

Recently, the advent of living carbocationic polymerization [5–8] has enabled the synthesis of PIB-based triblock copolymers [9–15] and a large number of new polymers of sophisticated architecture, such as star-branched polymers [16, 17], star-branched block copolymers [15–18], and telechelic polymers [19, 20], based upon isobutylene (IB) and other monomers inaccessible through living anionic polymerization. The new living carbocationic polymerization is based upon "cation stabilization," brought about either by careful selection of a counterion of suitable nucleophilicity [21] or by addition to the polymerization mixture of a Lewis base, i.e., an electron donor [7, 8, 21]. Cation stabilization is most readily observed by a dramatic decrease in the overall rate of polymerization, and is most often attributed to the formation of an equilibrium between a large number of dormant covalent (reversibly terminated) or onium chain ends and a small number of active ion pairs [8, 22, 23].

Of particular relevance to this paper is the work of Kaszas et al. [9, 10] who synthesized triblock copolymers of IB and styrene and other comonomers such as *p*-chlorostyrene [11], *p*-methylstyrene [12], *p-tert*-butylstyrene [13], and indene [14]. These authors reacted styrene with living PIB dications which were produced from a 1,4-*bis*-(2-methoxy-2-propyl)benzene/$TiCl_4$ initiating system, with *N,N*-dimethylacetamide as the electron donor, at −80°C in a 60/40 (v/v) mixture of hexanes/methyl chloride. They also demonstrated that the proton trap, 2,6-di-*tert*-butylpyridine, imparted a favorable effect upon the molecular weight distribution and tensile strength of the triblock copolymer product. Following the lead of Kaszas et al. [9, 10], we have developed and utilized a system for the living carbocationic polymeri-

zation of IB consisting of 1,4-*bis*-(2-chloro-2-propyl)benzene (dicumyl chloride) (DCC) or 1,3,5-*tris*-(2-chloro-2-propyl)benzene (TCC) as initiator, $TiCl_4$ as the co-initiator, and pyridine as the electron donor [8]. The solvent system consists of 60/40 (v/v) hexane/methyl chloride, which yields a homogeneous system with respect to the formed polymer, but not to the initiating complex, which persists throughout polymerization as a yellow precipitate.

The pyridine-based system yields PIBs of very narrow molecular weight distributions, and has been used very successfully for the synthesis of PIB telechelic ionomers [24], block copolymers [15], and block copolymer ionomers [25]. The kinetics of this system have been studied to help elucidate the effects of the various components in the system, and particularly to understand the effect of the time of addition of styrene to PIB chains on block copolymer structure and purity. The impetus for this study was the previous observation by ourselves [8, 15] and others [26–28] that for the living polymerization of IB, a deviation from living characteristics occurs at high monomer conversion.

EXPERIMENTAL

Polymerizations were carried out in a glove box under dry nitrogen. A representative polymerization procedure used to construct a single first-order plot was as follows: 400 mL methyl chloride, 1.09 mole IB, 1.94×10^{-3} mole DCC, 600 mL hexane, and 3.96×10^{-3} mole pyridine were added sequentially to a chilled 2 L three-necked round-bottomed flask, equipped with a mechanical stirrer. Methyl chloride and IB were condensed into chilled graduated cylinders before addition to the flask. The mixture was stirred for 30 minutes; then, 50 mL portions of the solution were transferred to chilled 25 × 250 mm culture tubes via a 50-mL volumetric pipet. With vigorous shaking, 1.82×10^{-3} mole $TiCl_4$ was rapidly injected into each stoppered culture tube to commence polymerization. Polymerizations in the various tubes were terminated at differing times, as dictated by experimental design, by the injection of 10 mL prechilled methanol. Fractional yield (Y) of polymer was determined gravimetrically, and the quantity $[M]_0/[M](= [IB]_0/[IB])$ was calculated as $1/(1 - Y)$.

Preparative block copolymerizations were carried out at −80°C using dry three-necked, round-bottomed flasks equipped with a mechanical stirrer. Detailed starting materials preparation, polymerization and polymer extraction procedures, and gel permeation chromatography (GPC) methods have been described [29].

Films were obtained by dissolving block copolymers in tetrahydrofuran, pouring the solutions into Teflon-coated bakeware, covering the pans with aluminum foil containing several small pinholes, and allowing the solvent to evaporate at room temperature under atmospheric pressure. Once dry to the touch, the films were removed from the pans and placed in a vacuum oven for a few days using initial temperatures in the 40–60°C range, under a slight vacuum to prevent bubbling of the films, and subsequently at 60°C using a high vacuum. Samples containing exceptionally high polystyrene contents (30 mol% and above) were eventually heated to 110°C and exposed to a high vacuum for 24 hours to ensure complete removal of tetrahydrofuran.

^{1}H-NMR spectra were obtained using a 200-MHz Bruker ACE-200 NMR spectrometer. Samples were prepared in CD_2Cl_2. Peak positions were reported against the internal reference of CH_2Cl_2 at 5.32 ppm.

Films for microscopy, prepared by compression molding at 180°C for 1 hour, were cryomicrotomed into sections of 800–1000 Å thickness. The PS domains were stained with RuO_4, and the sections were imaged using a Jeol 100CX instrument fitted with a Temscan attachment for scanning transmission electron microscopy. The microscope was operated at 100 kV.

Tensile properties were measured using an MTS Model 810 Universal Test Machine. Microdumbbell samples possessing a gauge length of 11.00 mm and a width of 1.54 mm were stamped from films ranging in thickness from 0.25 to 1.0 mm. A 100-lb load cell with a 100-lb load range cartridge and a 10-in. displacement cartridge were used in conjunction with a 1-mm/s continuous strain rate to obtain tensile data.

DMA spectra were obtained using a Seiko model SSC/5200H dynamic mechanical spectrometer equipped with a DMS 210 tension module. Rectangular samples possessing gauge lengths of 20 mm and widths in the range of 0.5 to 0.8 mm were used for testing. Spectra were obtained by holding the frequency constant at 1 Hz and sweeping temperature.

RESULTS AND DISCUSSION

Kinetics of Living Isobutylene Polymerization

The living carbocationic polymerization initiation system reported in this paper consists of a di- (or tri-) cumyl chloride initiator, pyridine ([Pyr] = 2[DCC]) and an excess of the Lewis acid coinitiator $TiCl_4$. An excess of $TiCl_4$ is necessary since it forms a strong complex with pyridine and thus is not available to coinitiate the polymerization unless used in excess. The most obvious effects of the addition of pyridine are a dramatic decrease in the rate of polymerization and a narrowing of the molecular weight distribution (MWD) of the formed polymers. Figure 1 shows a GPC trace of PIB produced in the presence of pyridine (narrow distribu-

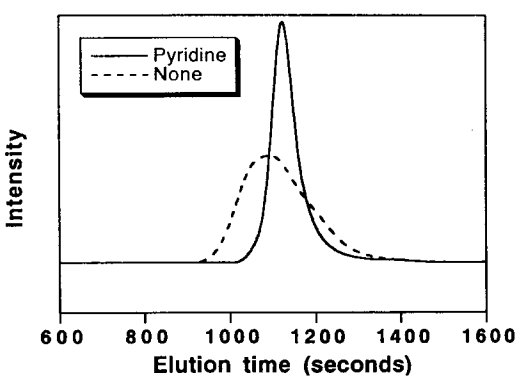

FIG. 1. GPC trace of PIB produced in the presence of pyridine (narrow distribution) compared to control polymerization conducted in the absence of pyridine.

tion) in comparison to a control polymerization which was conducted in the absence of pyridine. The control polymerization reached nearly 100% IB conversion within minutes; the living polymerization was terminated at a moderately high conversion after approximately 1 hour. The narrowness, symmetry, and perfect unimodality of the GPC trace of the living polymer demonstrates the extraordinary level of control over IB polymerization attainable using pyridine as an electron donor. As will be demonstrated, however, control such as this can only be achieved under a defined set of conditions.

To aid in the understanding and utilization of this system, the kinetics of the living carbocationic polymerization of IB using the DCC/$TiCl_4$/pyridine system were determined by monitoring the amount of polymer produced as a function of reaction time. Using a pyridine concentration equal to 2[DCC] and a $TiCl_4$ concentration equal to 10[Pyr], the data shown in Fig. 2 were obtained at −80°C. The linearity of the plots indicate that the polymerizations followed first-order kinetics with respect to monomer and that the number of actively growing chains remained invariant during a given polymerization. The plots also show that the rate of polymerization was strongly affected by the concentration of the initiation system, i.e., the apparent first-order rate constant, k_{app}, is a strong function of $[DCC]_0$, $[TiCl_4]$, and [Pyr]. The functional dependency of rate on concentration of the unitized initiation system was determined by plotting $\ln(k_{app})$ vs $\ln[DCC]_0$, as shown in Fig. 3. It should be noted that although the x-axis only plots $\ln[DCC]_0$, the other two components of the initiation system were also changed in direct proportion to $[DCC]_0$. The slopes of these lines show that the rate of polymerization is proportional to the 2.7 power of the initiation system concentration at −80°C and to the 2.2 power at −50°C.

Figure 4 illustrates the effect of temperature on the rate of polymerization. At equivalent initiation system concentration, the solid and open circles represent data obtained at −80 and −50°C, respectively. The data show that the rate of polymerization is faster at lower temperatures, indicating that the activation energy associated with the apparent rate constant is negative; for example, at $[DCC]_0 \approx 1.3 \times$

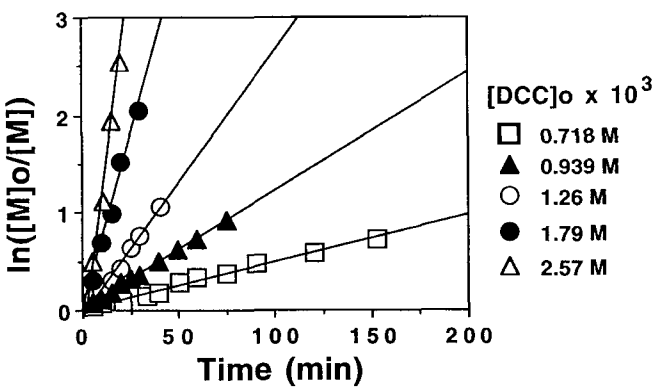

FIG. 2. Effect of initiation system concentration on the rate of polymerization of IB at −80°C in 60/40 hexane/methyl chloride. $[IB]_0$ = 1 M; $2[DCC]_0$ = [Pyr] = $[TiCl_4] \times 10^{-1}$.

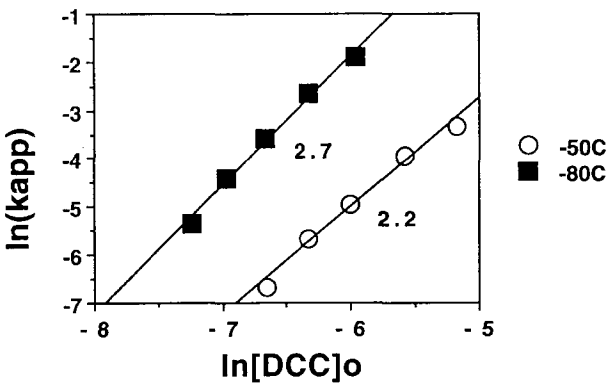

FIG. 3. Reaction order of initiation system concentration for polymerization of IB at −50 and −80°C in 60/40 hexane/methyl chloride. $[IB]_0$ = 1 M; $2[DCC]_0$ = [Pyr] = $[TiCl_4] \times 10^{-1}$.

10^{-3} M, the polymerization at −80°C is about seven times faster than the polymerization at −50°C. Since chain transfer and irreversible termination are not operating in the polymerization, these results point to an equilibrium between dormant and active chain carriers, which is exothermic in the direction of formation of the latter.

It was of interest to determine the contribution of each component of the initiation system to the overall reaction orders shown in Fig. 3. The dependence of the rate of polymerization on the concentration of $TiCl_4$ was determined by measuring the kinetic behavior of polymerizations conducted using various concentrations of $TiCl_4$ while keeping $[IB]_0$, $[DCC]_0$, and [Pyr] constant. The apparent first-order constants thus obtained are plotted as $\ln(k_{app})$ vs $\ln[TiCl_4]$ in Fig. 5, which shows a kinetic order with respect to $[TiCl_4]$ at −80°C equal to 2, which accounts for the largest part of the dependency of the overall initiation system. Second-order dependency with respect to $[TiCl_4]$ has been observed by others for similar systems [28, 30].

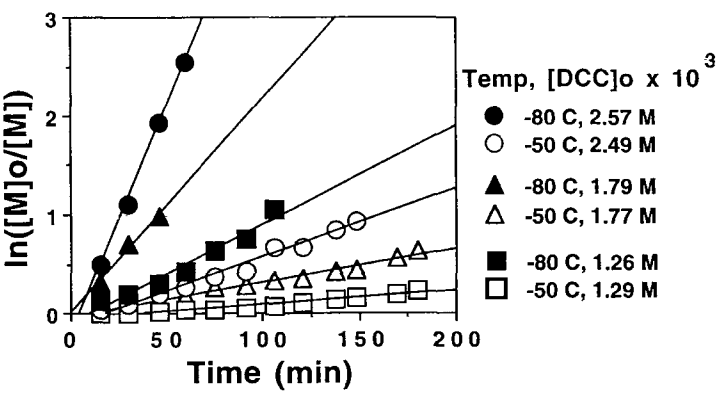

FIG. 4. Effect of temperature on the rate of polymerization of IB in 60/40 hexane/methyl chloride. $[IB]_0$ = 1 M; $2[DCC]_0$ = [Pyr] = $[TiCl_4] \times 10^{-1}$.

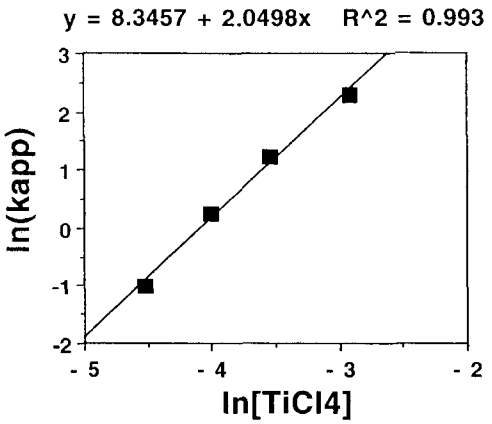

FIG. 5. Reaction order of $[TiCl_4]$ for polymerization of IB at −80°C in 60/40 hexane/methyl chloride. $[IB]_0 = 1$ M; $2[DCC]_0 = [Pyr] = 3.56 \times 10^{-3}$ M.

Using the same approach, it was found that the rate of polymerization varied with the first power of the DCC concentration. This indicates that the rate of polymerization is first order with respect to the concentration of actively growing chain ends, [R+], provided that the ratio $[R+]/[DCC]_0$ remains constant as $[DCC]_0$ is varied. The latter condition can be qualified by plotting $\ln([M]_0[M])/[DCC]_0$ vs time for several $[DCC]_0$, as shown in Fig. 6. The fact that all lines coincide shows that $[R+]/[DCC]_0$ is indeed a constant at a given temperature, and that the active chains are composed only of ion-paired species.

The effect of the concentration of pyridine was also studied in isolation, using concentrations of pyridine ranging, in terms of the ratio of moles of pyridine to moles of chain ends ($2[DCC]_0$), from 1/15 to 15/1 [Pry]/[chain ends]([CE]). Among the [Pyr]/[CE] ratios investigated, those below 1/3 yielded a deviation from linear-

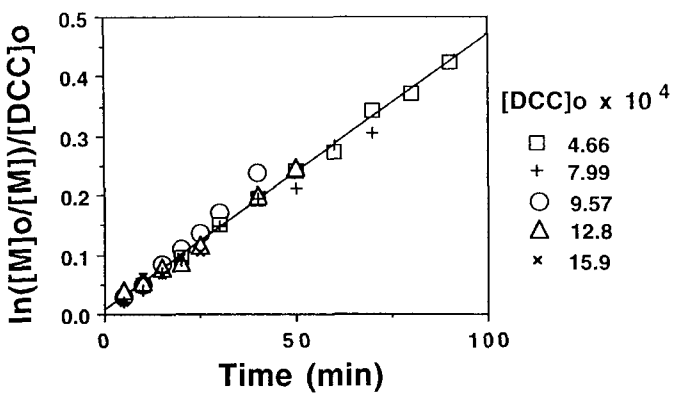

FIG. 6. Ln $([M]_0/[M])/[DCC]_0$ vs time for polymerization of IB for various DCC concentrations at −80°C in 60/40 hexane/methyl chloride. $[IB]_0 = 1$ M; $[Pyr] = 2.5 \times 10^{-3}$ M; $[TiCl_4] = 4.0 \times 10^{-2}$ M.

ity of first-order plots, which occurred very early in the polymerizations, indicating a loss over time of the number of propagating chains due to irreversible termination. At [Pry]/[CE] ratios above 1/3, first-order kinetic behavior was observed at −80°C, and the measured apparent rate constants were plotted as $\ln(k_{app})$ vs ln [Pyr] in Fig. 7. The data show that the dependence of the rate of polymerization on pyridine concentration at −80°C is −0.28. Other than the fact that it is negative, which is consistent with the retarding effects of pyridine, and that the value correlates well with the overall dependency of the unitized initiation system, no particular significance has been placed on this fractional negative power, and it is not known how this value changes with temperature.

Time of Addition of Styrene to Living PIB Chains

The foregoing kinetic investigations were done in part to elucidate the time required to grow living PIB dications in preparation for styrene addition during the synthesis of triblock copolymers. Previous observations have shown that the living characteristics of IB polymerization are rapidly lost after the monomer conversion reaches a certain critical value, dependent upon temperature, within the high conversion regime [8]. This phenomenon is illustrated in Fig. 8, which is a so-called "livingness" plot, i.e., a plot of $-\ln(1 - DP_n[I]_o/[M]_0)$ vs time, the linearity of which is both a necessary and sufficient condition for living polymerization behavior [31] (DP_n = number-average degree of polymerization, I = DCC or TCC). It will be noted that IB polymerizations in the presence of pyridine at −50 and −80°C are indeed living up to about 90% conversion. Around that point, however, there is observed a dramatic deviation from livingness, and it is apparent that the living character is sustained to slightly higher conversions at the lower temperature. Loss of living character also shows up as a broadening of the MWD, observable in GPC chromatograms of aliquots removed from a polymerization mixture over time. In Fig. 9 it is clear that living character was maintained for a polymerization time up to 1.5 hours; however, by 2 hours characteristic broadening had become apparent,

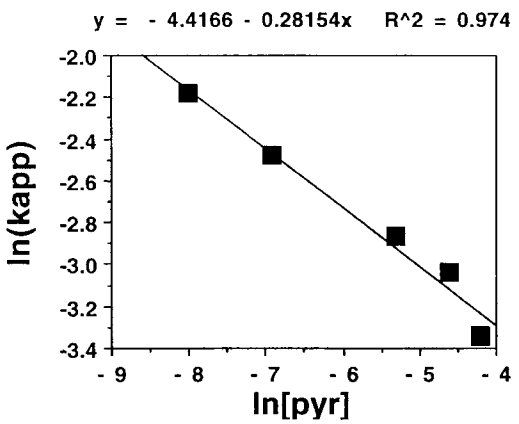

FIG. 7. Reaction order of [Pyr] for polymerization of IB at −80°C in 60/40 hexane/methyl chloride. $[IB]_0$ = 1 M; $[DCC]_0 = 1.0 \times 10^{-3}$ M; $[TiCl_4] = 4.0 \times 10^{-2}$ M.

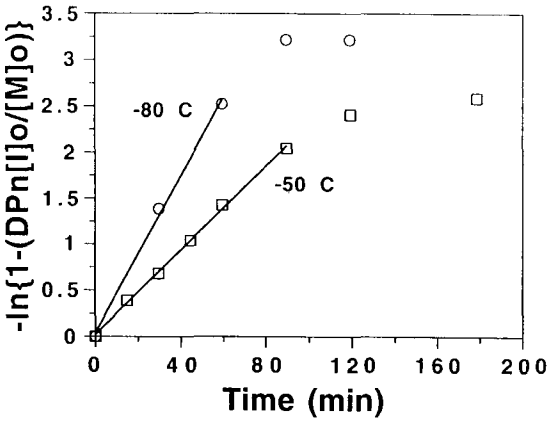

FIG. 8. $-\text{Ln}\ (1 - DP_n[I]_0/[M]_0)$ vs time for polymerization of IB at -50 and $-80°C$ in 60/40 hexane/methyl chloride. $[IB]_0 = 1$ M; $3[TCC]_0 = [Pyr] = 8.4 \times 10^{-3}$ M; $[TiCl_4] = 4.2 \times 10^{-2}$ M $(-50°C)$. $[IB]_0 = 1.32$ M; $2[DCC]_0 = [Pyr] = 7.4 \times 10^{-3}$; $[TiCl_4] = 3.7 \times 10^{-2}$ M $(-80°C)$.

and by 4 hours the product was contaminated with substantial amounts of low molecular weight material.

In view of the available evidence, others have suggested [28] and we also believe [29] that the deviation from livingness and concomitant broadening of the MWD are due to unimolecular β-proton elimination from growing chain ends. The low molecular weight tail seen in the GPC chromatograms of Fig. 9 is due to low molecular weight PIB chains initiated by the eliminated protons. Whether this reaction is accelerated by the depletion of monomer, or whether its rate is zero order with respect to monomer concentration, it becomes relatively more important as the rate of propagation diminishes at high conversions. Regardless of this question, β-proton elimination represents a critical problem for block copolymer synthe-

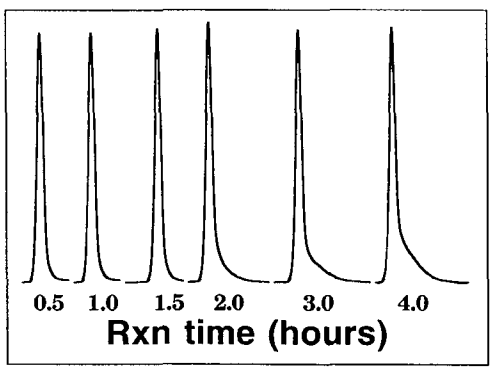

FIG. 9. GPC traces acquired as a function of reaction time for polymerization of IB at $-80°C$ in 60/40 hexane/methyl chloride. $[IB]_0 = 1$ M; $2[1,3\text{-}bis(2\text{-chloro-2-propyl})\text{-}5\text{-}tert\text{-butylbenzene}]_0 = [Pyr] = [TiCl_4] \times 10^{-1}$.

sis. Addition of styrene too late in time may result in the formation of block copolymer samples contaminated with AB block architectures and homopolymers. Conversely, an addition of styrene that is too early, i.e., occurring at a time when a significant fraction of the IB remains, may result in the formation of block copolymers lacking a distinct crossover from the PIB block to PS blocks as a result of random copolymerization between styrene and residual IB.

To illustrate the effect of the time of styrene addition on block copolymer sample composition, an IB polymerization reaction mixture containing DCC/pyridine was divided into three equivalent fractions, each of which was injected with a standard charge of $TiCl_4$ and allowed to polymerize to three different degrees of IB conversion prior to addition of styrene monomer. As shown in Fig. 10, addition of styrene at an IB reaction time far exceeding the time necessary for complete monomer consumption, indicated by the plateau in the PIB polymerization portion of the M_n vs time curve, caused a further, rapid increase in molecular weight. This, in conjunction with a shift to lower elution volumes in the GPC trace of the block copolymer relative to the GPC trace of PIB homopolymer removed from the reaction just prior to the addition of styrene (Fig. 11), indicates that styrene was added to PIB chains.

In Fig. 11 the GPC trace of the block copolymer shows a low molecular weight tail that is not present in the GPC trace of the parent PIB mid-block. This low molecular weight contaminant is PS homopolymer, initiated during the crossover to styrene polymerization by protons expelled from PIB chains. Extraction of this particular sample with methyl ethyl ketone (MEK) resulted in 13 wt% solubilization. The GPC trace of the MEK-soluble fraction (Fig. 12) shows two components, the block copolymer itself, indicating that it is slightly soluble in refluxing MEK, and a low molecular weight peak that was shown by ^1H NMR to be homo-PS. By comparing the integrated area under the homo-PS peak to the area

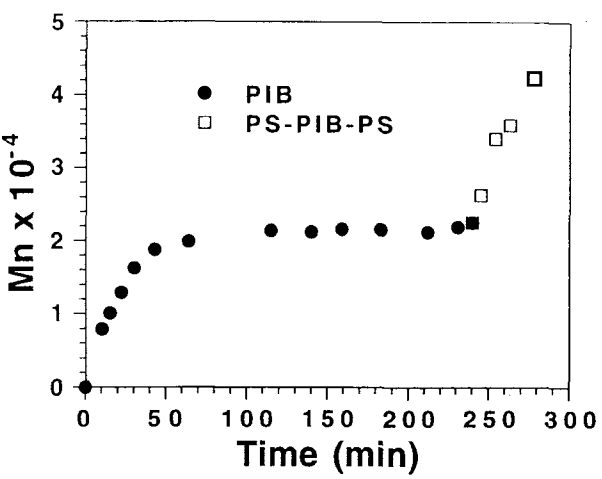

FIG. 10. M_n vs time for the block copolymerization of IB and styrene at −80°C in 60/40 hexane/methyl chloride, using an excessively long IB reaction time. $[IB]_0 = 1.2$ M; $2[DCC]_0 = [Pyr] = [TiCl_4] \times 10^{-1} = 3.8 \times 10^{-3}$ M; [styrene] = 0.4 M.

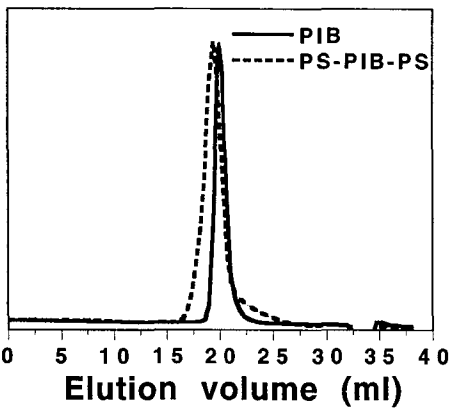

FIG. 11. GPC traces of the PIB mid-block and PS–PIB–PS block copolymer synthesized at −80°C in 60/40 hexane/methyl chloride, using an excessively long IB reaction time. $[IB]_0 = 1.2\,M$; $2[DCC]_0 = [Pyr] = [TiCl_4] \times 10^{-1} = 3.8 \times 10^{-3}\,M$; [styrene] = 0.4 M.

under the peak corresponding to PS–PIB–PS block copolymers, the amount of homo-PS was estimated to be 9.2 wt% of the total crude block copolymer sample.

The latter experiment demonstrates that a late addition of styrene causes contamination of the block copolymer with homo-PS. Kaszas et al. [9] showed that use of a proton trap such as 2,6-di-*tert*-butylpyridine (DtBuP) reduces the tendency toward homo-PS in similar systems, and Faust et al. [30] showed that DtBuP favorably influences the cationic homopolymerization of styrene using a 2,4,4-trimethyl-2-pentyl chloride/$TiCl_4$ initiating system. These observations support the hypothesis that homo-PS is initiated primarily by protons that are expelled from growing chains during the late stages of formation of the PIB block.

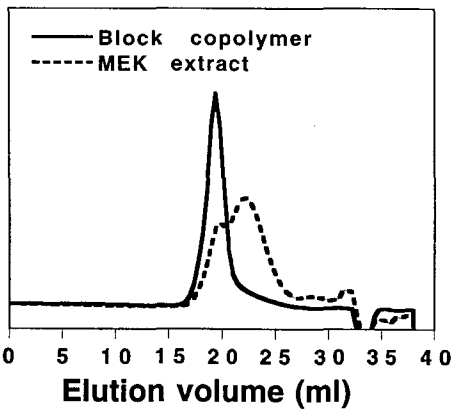

FIG. 12. GPC trace of the MEK-soluble fraction of the PS–PIB–PS block copolymer sample synthesized at −80°C in 60/40 hexane/methyl chloride, using an excessively long IB reaction time. $[IB]_0 = 1.2\,M$; $2[DCC]_0 = [Pyr] = [TiCl_4] \times 10^{-1} = 3.8 \times 10^{-3}\,M$; [styrene] = 0.4 M.

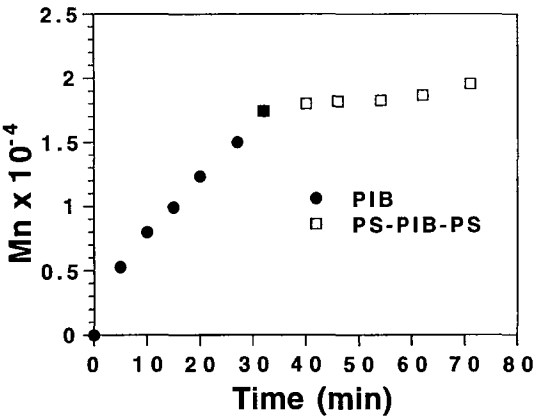

FIG. 13. M_n vs time for the block copolymerization of IB and styrene at −80°C in 60/40 hexane/methyl chloride, using an exceptionally short IB reaction time. $[IB]_0 = 1.2\,M$; $2[DCC]_0 = [Pyr] = [TiCl_4] \times 10^{-1} = 3.8 \times 10^{-3}\,M$; [styrene] = 0.4 M.

As shown in Fig. 13, addition of styrene to living PIB chains under conditions of intermediate IB conversion resulted in a subsequent retardation of the rate of polymerization. GPC traces of the reaction mixture, shown in Fig. 14, indicate very little increase in molecular weight after styrene addition, which also implies very slow propagation. The slow rate has been attributed to a simultaneous copolymerization between styrene and unreacted IB. Separate experiments have shown that simultaneous copolymerizations are slower than the rate of homo-PS block formation. These results suggest that an early addition of styrene leads to a "tapered" triblock copolymer possessing chain sections characterized by a gradual crossover from one to the other homopolymer.

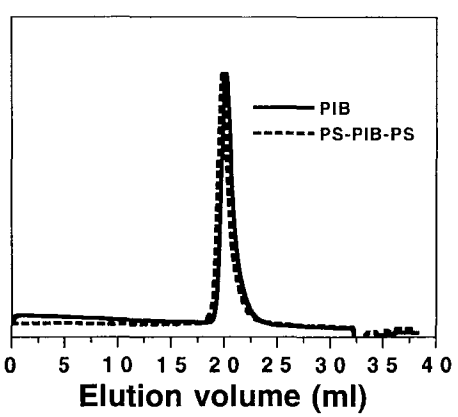

FIG. 14. GPC traces of the PIB mid-block and PS–PIB–PS block copolymer synthesized at −80°C in 60/40 hexane/methyl chloride, using an exceptionally short IB reaction time. $[IB]_0 = 1.2\,M$; $2[DCC]_0 = [Pyr] = [TiCl_4] \times 10^{-1} = 3.8 \times 10^{-3}\,M$; [styrene] = 0.4 M.

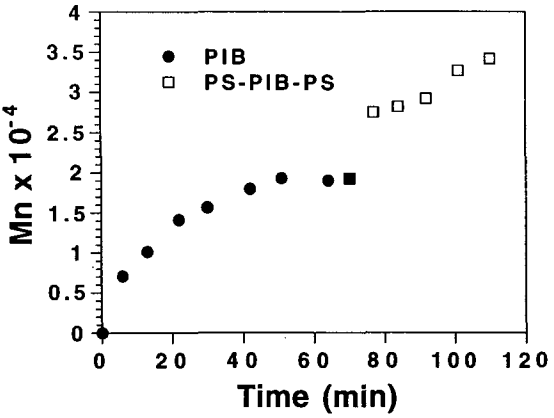

FIG. 15. M_n vs time for the block copolymerizatin of IB and styrene at −80°C in 60/40 hexane/methyl chloride, using an IB reaction time corresponding to nearly complete IB conversion. $[IB]_0$ = 1.2 M; $2[DCC]_0$ = [Pyr] = $[TiCl_4] \times 10^{-1} = 3.8 \times 10^{-3}$ M; [styrene] = 0.4 M.

Figure 15 demonstrates results from a block copolymerization in which styrene was added at the "proper" time, i.e., the latest time (highest possible conversion of IB) consistent with preservation of the living character of the PIB chains. In practice, this corresponds closely with the onset of the PIB molecular weight plateau that may be observed in Figs. 9 and 15. In Fig. 15 it will be noted that styrene addition at this point resulted in an abrupt increase in molecular weight, and that the GPC trace (Fig. 16) was shifted considerably toward lower elution volumes, indicating block copolymer formation. In this particular instance, the MWDs of the PIB block and the block copolymer were determined to be 1.19 and 1.25,

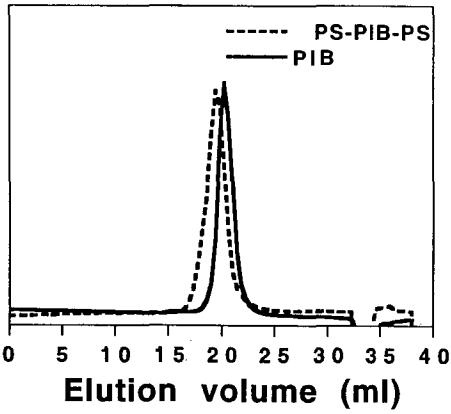

FIG. 16. GPC traces of the PIB mid-block and PS–PIB–PS block copolymer synthesized at −80°C in 60/40 hexane/methyl chloride, using an IB reaction time corresponding to nearly complete IB conversion. $[IB]_0$ = 1.2 M; $2[DCC]_0$ = [Pyr] = $[TiCl_4] \times 10^{-1} = 3.8 \times 10^{-3}$ M; [styrene] = 0.4 M.

respectively, and the amount of homo-PS contamination was estimated to be much less than that observed with a purposefully late time of addition of styrene.

Morphology and Properties of Triblock Copolymers

From the previous section it is clear that the time of styrene addition is critical to the synthesis of triblock copolymers that are uncontaminated with homopolymers and diblocks. Examination of the morphology of the resulting triblock copolymers is an excellent means of critically accessing the effectiveness of the synthetic method since the production of a highly ordered dual-phase morphology requires a very uniform molecular architecture with minimal contamination. Figure 17 is a transmission electron micrograph of a PS-PIB-PS block copolymer synthesized using

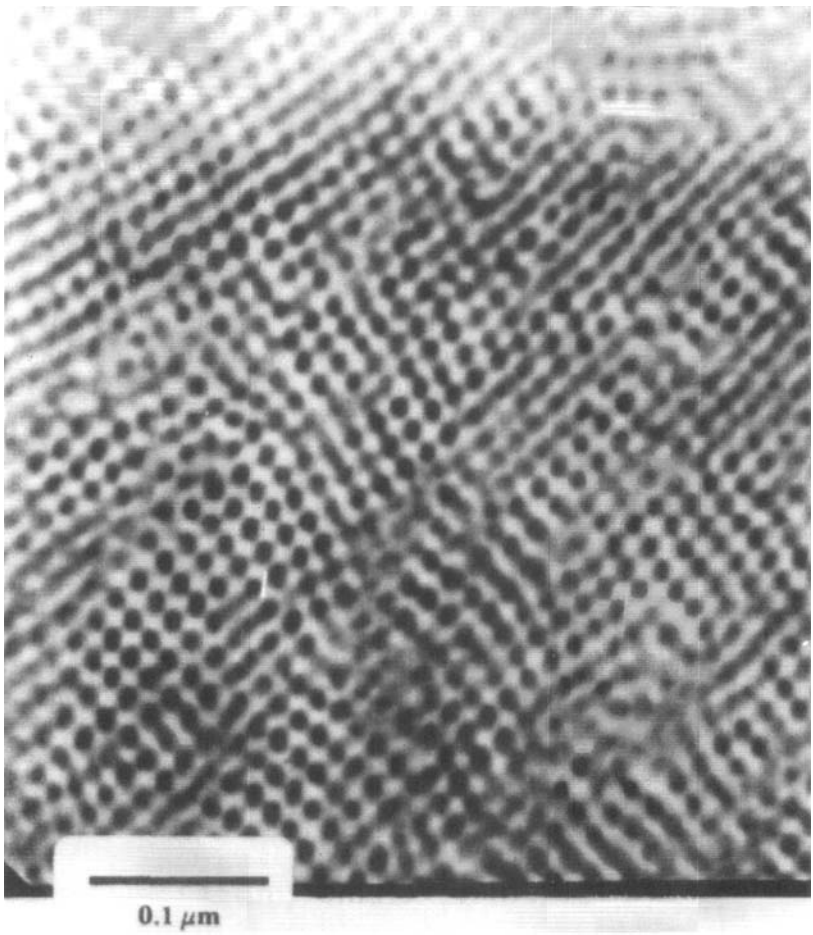

FIG. 17. Transmission electron micrograph of a PS-PIB-PS block copolymer synthesized at −80°C in 60/40 hexane/methyl chloride, using an IB reaction time corresponding to 91% IB conversion.

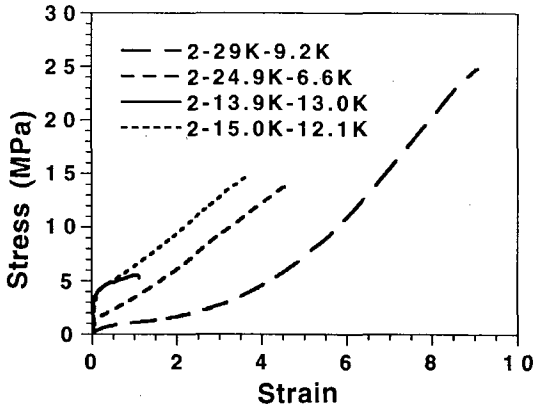

FIG. 18. Stress–strain curves for PS–PIB–PS block copolymers of various compositions.

the polymerization system described in this paper, in conjunction with the proton trap DtBuP, and an IB reaction time corresponding to 91% conversion, based on the molecular weight of the PIB mid-block and the assumption of 100% initiation efficiency. It is clear that the block copolymer sample possesses a heterogeneous morphology consisting of cylindrical PS domains (dark) dispersed within a matrix of PIB (light). The PS cylinders are aligned with their long axes parallel to one another, and they may be observed to form a hexagonal array. The highly ordered nature of the sample attests to the utility of this polymerization system and the effectiveness of the carefully timed addition of styrene.

The physical properties of PS–PIB–PS block copolymers were consistent with the observed dual-phase morphology. A series of A–B–A triblock copolymers was synthesized in which the PIB and PS block lengths were varied to yield a range of properties. Figure 18 depicts stress–strain curves for four triblock copolymers which

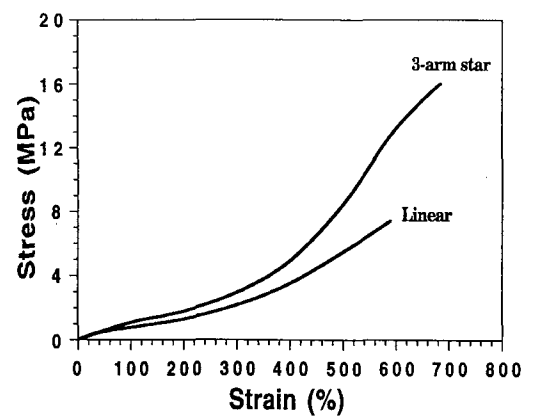

FIG. 19. Stress–strain curves of two-arm (linear) and three-arm star block copolymers with virtually identical arm compositions consisting of a PIB segment of 12.3K g/mol and PS segments of 4K g/mol.

are representative of the range of properties observed. Sample designations in the figure consist of three numbers: the first number, which in all cases is a 2, indicates a two-arm (linear) triblock; the second number indicates the PIB arm molecular weight (for a linear sample, equal to one-half of the entire PIB block molecular weight); and the third number indicates the molecular weight of the PS blocks. It may be observed that the 2-29K-9.2K sample yielded a tensile strength of 24 MPa and elongation of 900%, which represent excellent strength and toughness for a TPE. When both the PIB and PS block lengths were decreased, e.g., sample 2-24.9K-6.6K, the properties were observed to diminish. More importantly, when the relative PS content was increased, e.g., samples 2-13.9K-13.0K and 2-15.0K-12.1K, a dramatic change occurred in the tensile properties, which were characterized by a significantly increased modulus and a yield point followed by either a short draw and immediate break (2-13.9K-13.0K) or a period of draw combined with some degree of elastic extension (2-15.0K-12.1K). Thus, for PS–PIB–PS block copolymers, it appears that the optimum PS content for elastomeric properties is approximately 22–25 wt%; increases in PS content beyond this range apparently produces a semicontinuous PS phase, whose fracture leads to the observed yield points.

To understand the effect of molecular architecture, a comparison was made between a two-arm (linear) and a three-arm star block copolymer, each of which had virtually identical arm compositions consisting of a PIB segment of 12.3K g/mol and PS segments of 4K g/mol. Figure 19 shows stress–strain curves for these two samples. The three-arm star copolymer proved to be more than twice as strong as its linear counterpart. The additional network junction points contributed by the covalent hub of the star are apparently very important for strength, especially so for these samples which have a very short PS outer block. It is quite interesting that, in contrast to the strength, the elongation was hardly affected by molecular architecture. This is understandable since the span length (i.e., the length of two arms) is the same for both samples.

Dynamic mechanical properties of PS–PIB–PS block copolymers were also studied as a function of composition, and the results for a representative elastomeric

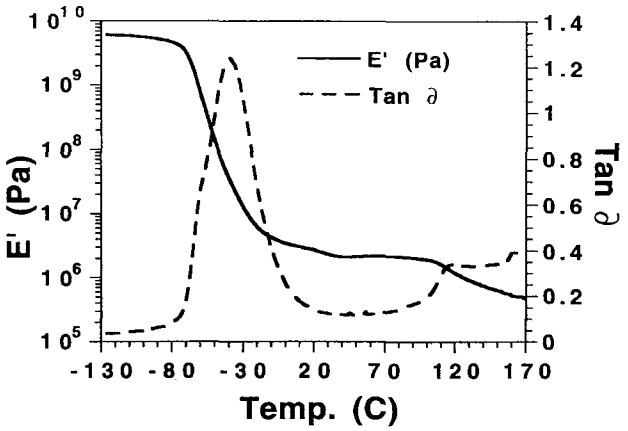

FIG. 20. Dynamic mechanical properties of a PS–PIB–PS block copolymer with PIB mid-block of 58K g/mol and PS outer blocks of 9.2K g/mol.

sample (2-29K-9.2K) are shown in Fig. 20. It may be seen that the dynamic storage modulus showed a glassy region below −65°C, and that beginning at −65°C, which corresponds with the T_g of the sample measured calorimetrically, the sample softened and the modulus decreased. However, the modulus drop was gradual with temperature, and the rubbery plateau value of the elastic modulus was reached between 0 and 20°C. The rubbery plateau extended to approximately 100°C, which corresponds to the T_g of the polystyrene block. The tan δ curve shows the well-known complex behavior of the low temperature transition of PIB. A mechanical relaxation was observed to begin at −65°C, which corresponds to the T_g of PIB. However, superimposed upon it was a slightly higher temperature relaxation that is broader and of much greater intensity; together, the two relaxations presented a half width at half maximum on the order of 50°C. This is considerably broader than that found in diene-based TPEs, and it demonstrates the greater low temperature mechanical damping properties that PS–PIB–PS block copolymers possess.

CONCLUSIONS

The new living carbocationic polymerization has enabled the synthesis of PIB-based triblock copolymers, and a large number of new polymers of various architectures, created from monomers that are not polymerizable by living anionic polymerization. Of the many initiation systems that have been reported for the living polymerization of IB, the DCC (or TCC)/$TiCl_4$/pyridine system yields an extraordinary level of control over the polymerization, and when used properly, will consistently yield PIB of predictable molecular weight and narrow, unimodal molecular weight distribution.

The kinetics of the DCC/$TiCl_4$/pyridine system have been found to be first order in IB concentration, first order in the concentration of initiating sites, second order in $TiCl_4$ concentration, and a negative fractional order with respect to the pyridine concentration. Importantly, the rate of polymerization was found to decrease with increasing temperature, indicating an equilibrium between dormant, covalent and active, ionized chain ends.

Regardless of the particular initiation system used, the livingness of IB polymerizations is not nearly so ideal as living anionic polymerizations. With the current technology, living IB polymerizations appear to be universally characterized by a deviation from living characteristics at high monomer conversions, due most probably to β-proton elimination. In view of this, successful synthesis of PS–PIB–PS block copolymers requires very careful timing of the addition of styrene to living PIB dications. Addition of styrene at an IB reaction time significantly exceeding the time necessary for complete IB consumption results in contamination of the product with a substantial amount of homo-PS; conversely, addition at an intermediate IB conversion results in slow copolymerization between IB and styrene and most likely the formation of a tapered block copolymer. Addition of styrene at an IB conversion of about 90% results in well-defined block copolymers, and a proton trap can be used to lessen the impact of slight errors in timing.

Used in the prescribed manner, the DCC/$TiCl_4$/pyridine system can yield well-defined PS–PIB–PS block copolymers which display ordered, phase-separated morphologies, and behave as TPEs. Dynamic mechanical spectroscopy on represen-

tatives samples has revealed two glass transitions with a broad rubbery plateau extending from about 0 to 100°C, and tensile strengths of up to 25 MPa and elongations to 1000% have been observed.

ACKNOWLEDGMENTS

The authors wish to acknowledge Shell Development Company, Houston, Texas, for support of this research. Special thanks are extended to Dr. Michail Masse for his helpful interpretations of block copolymer morphology and dynamic mechanical properties. The authors are also grateful to GE Plastics, The General Electric Company, Mount Vernon, Indiana, for fellowship support of Bret J. Chisholm.

REFERENCES AND NOTES

[1] C. P. O'Farrell and G. E. Serniuk, U.S. Patent 3,836,511 (1974) to Esso Research and Engineering Co.
[2] R. F. Storey, S. E. George, and M. E. Nelson, *Macromolecules*, *24*, 2920 (1991).
[3] G. Holden and N. R. Legge, in *Thermoplastic Elastomers* (N. R. Legge, G. Holden, and H. E. Schroeder, Eds.), Hanser Publishers, New York, 1987, Chapter 3.
[4] Marketed by Shell Chemical Co.
[5] M. Miyamoto, M. Sawamoto, and T. Higashimura, *Macromolecules*, *17*, 265 (1984).
[6] R. Faust and J. P. Kennedy, *J. Polym. Sci., Polym. Chem. Ed.*, *25*, 1847 (1987).
[7] G. Kaszas, J. E. Puskas, J. P. Kennedy, and C. C. Chen, *J. Macromol. Sci.—Chem.*, *A26*(8), 1099 (1989).
[8] R. F. Storey and Y. Lee, *J. Macromol. Sci.—Pure Appl. Chem.*, *A29*(11), 1017 (1992).
[9] G. Kaszas, J. E. Puskas, J. P. Kennedy, and W. G. Hager, *J. Polym. Sci., Polym. Chem. Ed.*, *29*, 427 (1991).
[10] J. E. Puskas, G. Kaszas, J. P. Kennedy, and W. G. Hager, *Ibid.*, *30*, 41 (1992).
[11] J. P. Kennedy and J. Kurian, *Ibid.*, *28*, 3725 (1990).
[12] Y. Tsunogae and J. P. Kennedy, *Polym. Bull.*, *27*, 631 (1992).
[13] J. P. Kennedy, M. Meguyira, and B. Keszler, *Macromolecules*, *24*, 6572 (1991).
[14] J. P. Kennedy, S. Midha, and Y. Tsunogae, *Ibid.*, *26*, 429 (1993).
[15] R. F. Storey, B. J. Chisholm, and Y. Lee, *Polymer*, *34*(20), 4330 (1993).
[16] B. Ivan and J. P. Kennedy, *J. Polym. Sci., Polym. Chem. Ed.*, *28*, 89 (1990).
[17] H. Shohi, M. Sawamoto, and T. Higashimura, *Macromolecules*, *24*, 4926 (1991).
[18] S. Kanaoka, M. Sawamoto, and T. Higashimura, *Ibid.*, *24*, 2309 (1991).
[19] M. Sawamoto, T. Enoki, and T. Higashimura, *Ibid.*, *20*, 1 (1987).

[20] A. V. Lubnin, J. P. Kennedy, and B. L. Goodall, *Polym. Bull.*, *30*, 19 (1993).
[21] T. Higashimura, S. Aoshima, and M. Sawamoto, *Makromol. Chem., Macromol. Symp.*, *13/14*, 457 (1988).
[22] G. Kaszas, J. E. Puskas, C. C. Chen, and J. P. Kennedy, *Macromolecules*, *23*, 3909 (1990).
[23] B. Ivan and J. P. Kennedy, *Ibid.*, *23*, 2880 (1990).
[24] R. F. Storey and Y. Lee, *J. Polym. Sci., Polym. Chem. Ed.*, *29*, 317 (1991).
[25] R. F. Storey, B. J. Chisholm, and Y. Lee, In Preparation.
[26] B. Wang, M. Mishra, and J. P. Kennedy, *Polym. Bull.*, *17*, 205 (1987).
[27] G. Kaszas, J. E. Puskas, and J. P. Kennedy, *Ibid.*, *18*, 123 (1987).
[28] M. Gyor, H. C. Wang, and R. Faust, *J. Macromol. Sci.—Pure Appl. Chem.*, *A29*, 639 (1992).
[29] R. F. Storey and B. J. Chisholm, *Macromolecules*, *26*, 6727 (1993).
[30] Z. Fodor, M. Gyor, H.-C. Wang, and R. Faust, *J. Macromol. Sci.—Pure Appl. Chem.*, *A30*(5), 349 (1993).
[31] S. Penczek, P. Kubias, and R. Szymanski, *Makromol. Chem., Rapid Commun.*, *12*, 77 (1991).